

Decomposition Behavior of Polyurethanes via Mathematical Simulation

WALLY L. CHANG

Witco Corporation, Polymer R&D Laboratories, Chicago, Illinois 60638

SYNOPSIS

A series of polyurethane elastomers with different hard-segment contents of 24% (M24), 34% (M34), 50% (M50), and 100% (M100) have been investigated through thermogravimetric analysis (TGA) measurement and mathematical simulation. The fourth-order Runge-Kutta method was used to solve the differential equations, and the solutions were obtained by running a written computer program. The activation energy and the frequency factor of polyurethane decomposition can be obtained by only one nonisothermal measurement of TGA. The same values of the activation energy and the frequency factor were obtained using the different constant heating rates under air for the elastomer with a hard-segment content of 34%. The activation energy decreases as the hard-segment content of polyurethanes increases. The polyurethane materials can be used at room temperature for several millennia without failure through lifetime calculation. Comparison of the values of $t_{1/2}$, the heat stability of polyurethanes decreases in the following order: M24 > M34 > M50 > M100; this phenomenon can be explained due to the heat instability of the urethane group. The highest concentration of the urethane group in the M100 structure results in the worst heat stability. © 1994 John Wiley & Sons, Inc.

INTRODUCTION

Thermogravimetric analysis (TGA) has been widely used to investigate the decomposition characteristics of many materials. With proper experimental procedures, information about the kinetics of decomposition and in-use lifetime projections can be obtained. In many polymer applications, the ability to predict product lifetime is valuable because the costs of premature failure in actual end use can be high. TGA provides a method for accelerating the lifetime testing of polymers so that short-term experiments can be used to predict in-use lifetime.

Polyurethanes are excellent polymer materials for a wide variety of applications because of their outstanding physical properties. Variation in hardness of polyurethane products can be easily obtained by changing the hard-segment content in the structure. In order to understand the decomposition kinetics and estimated lifetime of polyurethanes, a series of MDI-based polyurethane elastomers with different

hard-segment contents have been studied in this article.

EXPERIMENTAL

Elastomer Preparation

Prior to elastomer preparation, the polyester glycol and the 1,4-butanediol (1,4-BD) were vacuum dehydrated to a moisture content of less than 0.03 wt %. 4,4'-Diphenylmethane diisocyanate (MDI) was handled per manufacturer's recommendation and was decanted and filtered at 50°C to eliminate any insolubles. The materials are listed in Table I.

All MDI-based elastomers with hard-segment contents of 24, 34, 50, and 100% were made by following standard prepolymer production, i.e., a calculated amount of dry poly(butylene adipate) glycol with a molecular weight of 2000 (PBAG-2000) at 70°C was added to MDI at 50°C with stirring under a nitrogen blanket. The prepolymer was then synthesized for 3 h at a controlled temperature of 80°C. NCO% analysis confirmed the finished prepolymer,

Table I Designation of Materials and Products

Designation	Description	Supplier
1,4-BD	1,4-Butanediol	Arco
Fomrez 44-58	PBAG-2000	Witco
MDI	4,4'-Diphenylmethane Diisocyanate	BASF
Elastomer	Description	Hard Segment %
M24	MDI/44-58/1,4-BD	24
M34	MDI/44-58/1,4-BD	34
M50	MDI/44-58/1,4-BD	50
M100	MDI/1,4-BD	100

which was then extended with 1,4-BD. The mixture was cast into ASTM plaque and button molds, preheated to 110°C, cured at 120°C for 1 h in mold, and postcured at 100°C for at least 16 h. The cured elastomer was then conditioned at room temperature for a minimum of 1 week prior to testing. The I.I. [isocyanate index, (NCO/OH) × 100] was 105 for all elastomers. The hard-segment content can be determined using the following equation and the designation is listed in Table I.

Hard segment %

$$= \frac{(\text{MDI} + 1,4\text{-BD})}{(\text{MDI} + 1,4\text{-BD} + \text{PBAG-2000})} \times 100\% \quad (1)$$

Instrumental Method

A TA 951 TGA Analyzer with Thermal Analyst 2100 Control/Acquisition Data System was used to obtain the decomposition thermograms. The computer programs developed were run on an IBM compatible PC.

RESULTS AND DISCUSSION

Decomposition Order, Activation Energy, and Frequency Factor

From Maximum Decomposition Rate Temperature (T_m) by Several Nonisothermal Measurements of TGA

The decomposition rate can be described by an equation:¹

$$d\alpha/dt = k(1 - \alpha)^n \quad (2)$$

where $d\alpha/dt$ = the decomposition rate, α = the degree of decomposition, n = the empirical order of

decomposition, k = the decomposition rate constant which can be expressed by Arrhenius equation:

$$k = A \cdot \exp(-E/RT) \quad (3)$$

where A = the frequency factor (1/s), E = the activation energy (J/mol), R = the gas constant (8.314 J/mol · °K), and T = the Kelvin temperature (°K). Equation (2) can be rewritten by substituting Eq. (3) in Eq. (2):

$$d\alpha/dt = A \cdot \exp(-E/RT) \cdot (1 - \alpha)^n \quad (4)$$

Experiments in thermal analysis are carried out at a constant heating rate, q (°C/s) = dT/dt . Equation (4) can, thus, be written in the form:

$$d\alpha/dT = (A/q) \cdot \exp(-E/RT) \cdot (1 - \alpha)^n \quad (5)$$

In TGA measurements, the degree of decomposition can be calculated as follows:^{2,3}

$$\alpha = \frac{(W_o - W)}{(W_o - W_f)} \quad (6)$$

where W , W_o , and W_f are the actual, initial, and final weights of the sample, respectively. The $d/dT(d\alpha/dT)$ can be obtained from Eq. (5):

$$\frac{d^2\alpha}{dT^2} = \left[\frac{E}{RT^2} - \frac{n}{(1 - \alpha)} \cdot \frac{d\alpha}{dT} \right] \cdot \frac{d\alpha}{dT} \quad (7)$$

or

$$\frac{d^2\alpha}{dT^2} = \left[\frac{E}{RT^2} - \frac{A}{q} \cdot \exp\left(-\frac{E}{RT}\right) \cdot n(1 - \alpha)^{n-1} \right] \times \frac{A}{q} \cdot \exp\left(-\frac{E}{RT}\right) \cdot (1 - \alpha)^n \quad (8)$$

If the temperature of TGA measurement increases during the decomposition, the decomposition rate, $d\alpha/dt$, will rise to a maximum value, then return to zero as the reactant is exhausted. The maximum decomposition rate occurs at a temperature T_m , defined by setting Eq. (8) equal to zero. The following equation can be obtained:

$$\frac{Eq}{RT_m^2} = A \cdot \exp\left(-\frac{E}{RT_m}\right) \cdot n(1-\alpha)_m^{n-1} \quad (9)$$

Eq.(9) can be further rearranged:

$$\ln\left(\frac{q}{T_m^2}\right) = -\frac{E}{RT_m} + \ln\left[\frac{ARn(1-\alpha)_m^{n-1}}{E}\right] \quad (10)$$

Equation (10) can be simplified if the decomposition kinetics is the first-order reaction ($n = 1$):

$$\ln\left(\frac{q}{T_m^2}\right) = -\frac{E}{RT_m} + \ln\left(\frac{AR}{E}\right) \quad (11)$$

Upon completion of constant heating rates of TGA measurements, $\ln(q/T_m^2)$ is plotted against $1/T_m$. The activation energy E and the frequency factor A can be determined from the slope and the intercept, respectively. This method has been widely used for DSC (differential scanning calorimetry) study in

reaction kinetics.⁴⁻⁸ Contrary to the theoretical approach, it is not very easy to obtain a smooth curve of $d\alpha/dt$ vs. temperature using this method for TGA. Hence, it is very difficult to determine the T_m (see Fig. 1). Therefore, this method is not suitable for the TGA study of decomposition kinetics.

From Isothermal Condition by One Measurement of TGA

Eq. (4) can be rearranged as the following equation if the temperature is constant:

$$\ln\left(\frac{d\alpha}{dt}\right) = n \cdot \ln(1-\alpha) + \left(-\frac{E}{RT} + \ln A\right) \quad (12)$$

From a plot of $\ln(d\alpha/dt)$ vs. $\ln(1-\alpha)$, the decomposition order n can be obtained from the slope. Unfortunately, it is very difficult to obtain the value of α from Eq. (6) because of the extremely long time necessary to obtain W_f .

From Nonisothermal Condition by One Measurement of TGA

Eq. (4) can also be rewritten in the following form:

$$\ln\left[\frac{(d\alpha/dt)}{(1-\alpha)^n}\right] = -\frac{E}{RT} + \ln A \quad (13)$$

MDI Elastomer Hard Segment 34 % under air

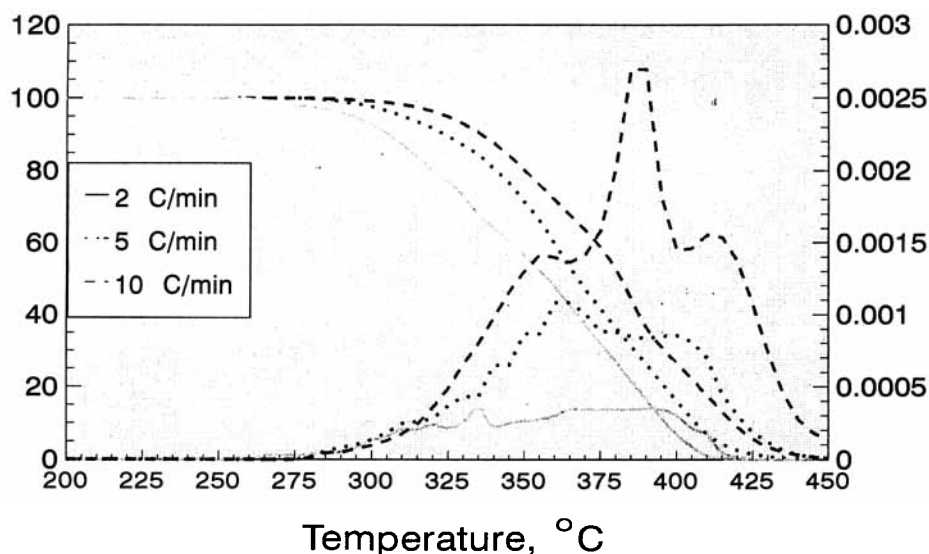


Figure 1 $(1-\alpha)$ % and $d\alpha/dt$ vs. temperature.

A plot of $\ln[(d\alpha/dt)/(1-\alpha)^n]$ against $1/T$ will yield a straight line fit of the data from which the decomposition order n can be selected. The slope of this line will provide the activation energy and the intercept can provide the frequency factor.^{9,10}

A MDI-based elastomer with a hard-segment content of 34% (M34) was run using TGA with a constant heating rate of 5°C/min and under air condition. As can be seen from Figure 2, only $n = 1$ gives a straight line and 1.24×10^5 J/mol of the activation energy as well as 2.74×10^7 1/s of the frequency factor were obtained. The same values of the reaction order, the activation energy, and the frequency factor were also obtained with constant heating rates of 2°C/min and 10°C/min, respectively. The activation energy and the frequency factor of MDI-based elastomers with the different hard-segment contents (M24, M34, M50, and M100) are summarized in Table II.

Mathematical Simulation

Experiment and Simulation

Equation (5) can be rewritten in the following form if $x = T$, $y = \alpha$, $C_1 = A/q$, and $C_2 = -E/R$, where C_1 and C_2 are constants:

$$\frac{dy}{dx} = C_1 e^{C_2/x} (1-y)^n \quad (14)$$

Unfortunately, Eq. (14) is a differential equation for which we cannot obtain an explicit solution. However, if initial conditions are given, we can generate a function that will approximate the solution to a given degree of accuracy. The procedure used to generate the function is usually called a numerical method for obtaining solutions for differential equations. A fairly simple technique for the numerical solution of a differential equation is Euler's method. Unfortunately, this technique can be very inaccurate. A method that usually gives good results and that requires no special formulas to start the problem is one known as the Runge-Kutta method. An efficient fourth-order Runge-Kutta method was used to solve the differential rate equation in this study. The method can be outlined very briefly as follows:¹¹

$$y' = f(x, y)$$

$$k_1 = \Delta x \cdot f(x_n, y_n)$$

$$k_2 = \Delta x \cdot f(x_n + \Delta x/2, y_n + k_1/2)$$

$$k_3 = \Delta x \cdot f(x_n + \Delta x/2, y_n + k_2/2)$$

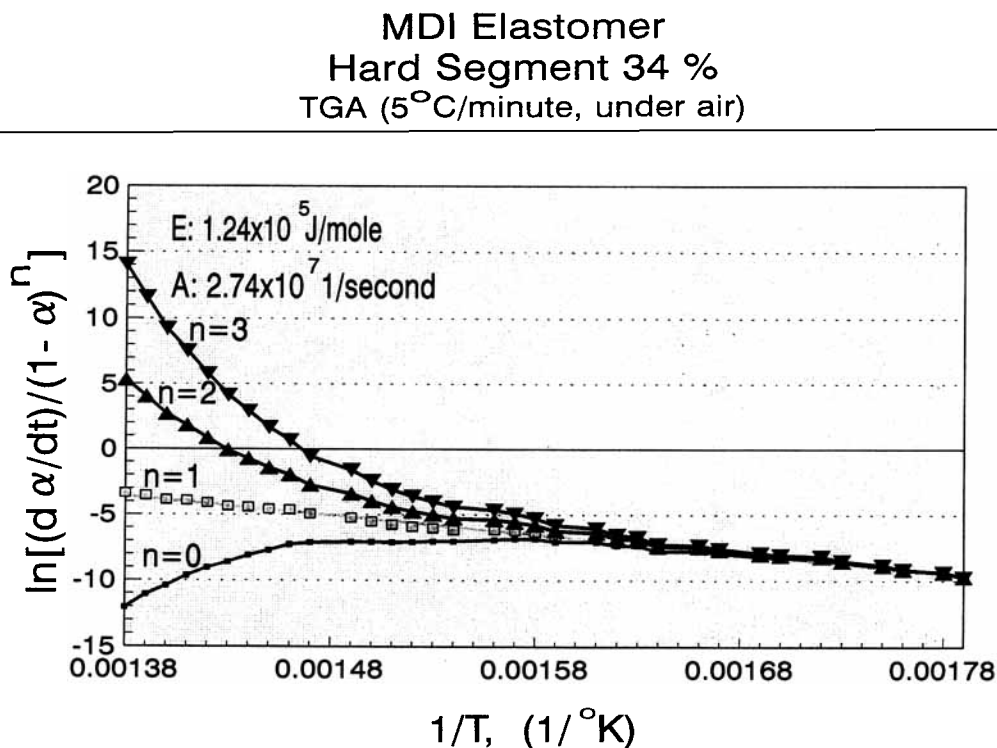


Table II The Decomposition Data of MDI-Based Elastomers via Simulation under Air: First-Order Decomposition Kinetics

Elastomer	H %	°C/min	E (J/mol)	A (1/s)	T_{max} , °C	T_1 , °C	T_2 , °C	T_2/T_1	S -index	$\alpha_m\%$	$(1 - \alpha)_m\%$
M24	24	5	1.26E + 05	3.41E + 07	383	357	410	1.08	0.5950	59.7	40.3
M34	34	0.01	1.24E + 05	2.74E + 07	247	230	264	1.07	0.5806	61.1	38.9
M34	34	0.1	1.24E + 05	2.74E + 07	289	269	309	1.07	0.5857	60.9	39.1
M34	34	1	1.24E + 05	2.74E + 07	338	314	361	1.08	0.5912	60.5	39.5
M34	34	5	1.24E + 05	2.74E + 07	377	351	404	1.08	0.5957	59.6	40.4
M34	34	10	1.24E + 05	2.74E + 07	396	368	424	1.09	0.5978	60.2	39.8
M34	34	20	1.24E + 05	2.74E + 07	416	386	445	1.09	0.6002	60.0	40.0
M34	34	30	1.24E + 05	2.74E + 07	428	397	458	1.09	0.6015	60.5	39.5
M34	34	50	1.24E + 05	2.74E + 07	443	413	475	1.09	0.6018	59.7	40.3
M50	50	5	1.17E + 05	1.22E + 07	361	334	388	1.09	0.5984	60.0	40.0
M100	100	5	1.03E + 05	2.01E + 06	333	305	361	1.10	0.6052	59.7	40.3

$$k_4 = \Delta x \cdot f(x_n + \Delta x, y_n + k_3)$$

$$y_{(n+1)} = y_n + \frac{1}{6}(k_1 + 2k_2 + 2k_3 + k_4)$$

Figure 3 shows $(1 - \alpha)\%$ and $d\alpha/dt$ vs. temperature by experiment and via mathematical simulation. It can be clearly seen that the simulation and actual experimentation curves match closely.

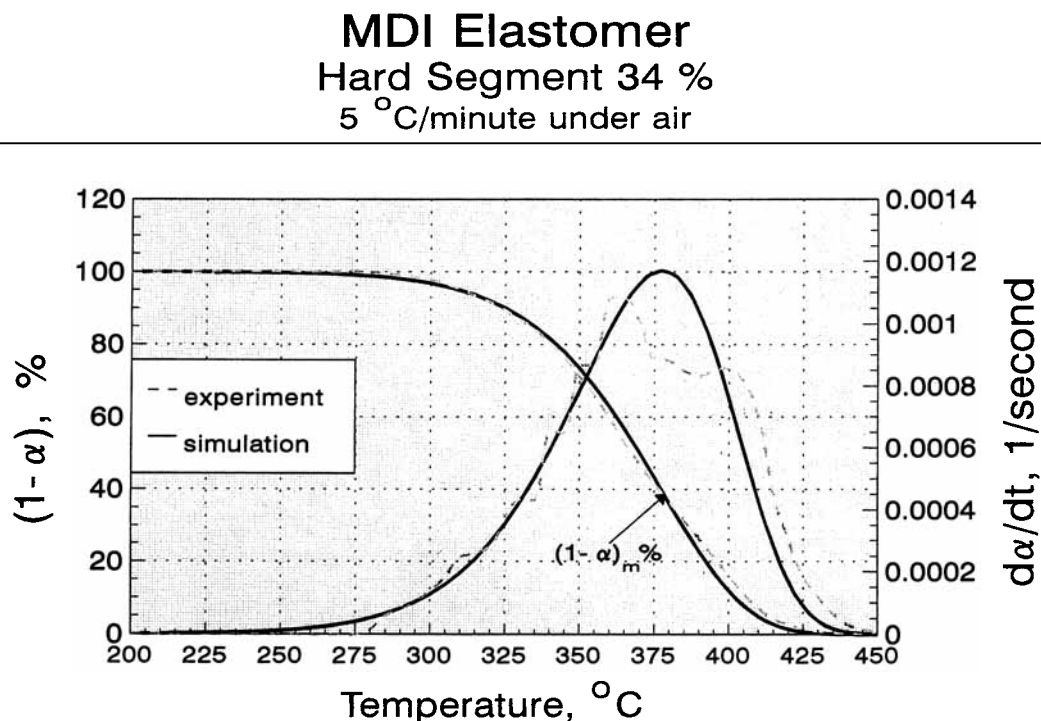
Reaction Order from the Shapes of the TGA Curves

The curves of $(1 - \alpha)\%$ and $d\alpha/dt$ vs. temperature can be generated via mathematical simulation using

the different n values. As seen from Figures 4 and 5, the experimental curves fit very closely to the simulated curve of $n = 1$.

TGA Curves of Different Heating Rates

Using the values of the activation energy (1.24×10^5 J/mol) and the frequency factor (2.74×10^7 1/s) of the M34 elastomer under air decomposition, a series of simulated curves from the different heating rates can be generated (see Fig. 6). T_m can also be obtained at the maximum decomposition rate. The data are listed in Table II.


Figure 3 $(1 - \alpha)\%$ and $d\alpha/dt$ via simulation.

MDI Elastomer
Hard Segment 34 %
under air

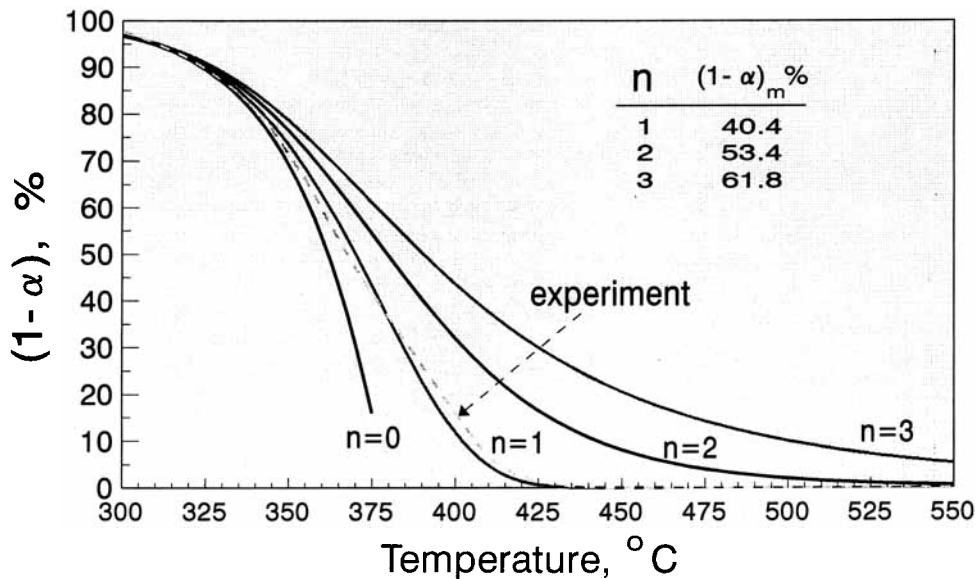


Figure 4 The shape of TGA curves based on decomposition order via simulation.

MDI Elastomer
Hard Segment 34 %
under air

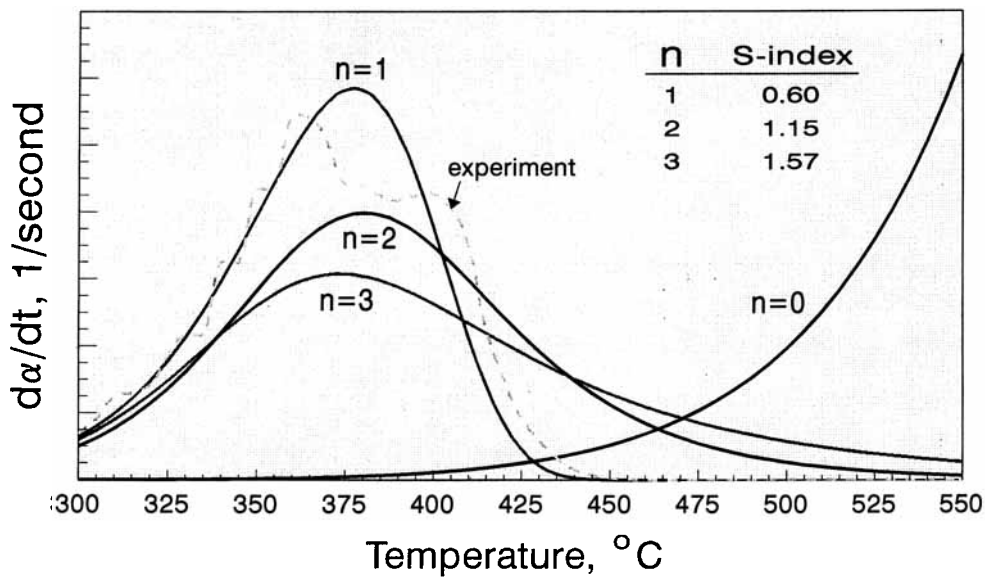


Figure 5 The shape of $d\alpha/dt$ curves based on decomposition order via simulation.

MDI Elastomer Hard Segment 34 % under air

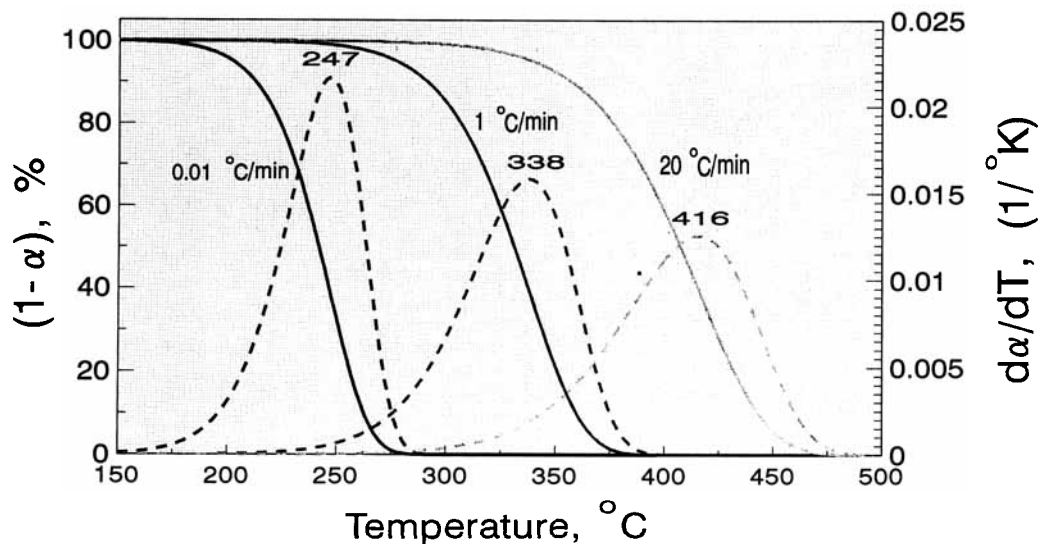


Figure 6 $(1 - \alpha)$ % and $d\alpha/dT$ via simulation.

Shape Index

Figure 5 implies that the corresponding differential thermal analysis peak becomes increasingly asymmetric as n is decreased from 2 to 1. To quantitatively describe the peak shape, a "shape index" was proposed by H. E. Kissinger.¹ Defined as the absolute value of the ratio of the slopes of tangents to the curve at the inflection points, the shape index can be expressed analytically as

$$S = \left| \frac{(d^2\alpha/dT^2)_1}{(d^2\alpha/dT^2)_2} \right| \quad (15)$$

where subscripts 1 and 2 refer to the value of these quantities at the inflection points, i.e., where

$$\frac{d^3\alpha}{dT^3} = 0$$

Figure 7 is generated using Eq. (7) and T_1 as well as T_2 (T_1 and T_2 are the temperatures at the first and second inflection points of the curve of $d\alpha/dT$ vs. temperature, respectively) can be obtained from the maximum points of $d^2\alpha/dT^2$ curve. All the values of T_1 , T_2 and T_2/T_1 are summarized in Table II. An average value of 1.08 of T_2/T_1 was obtained which shows the same value reported.¹ An average

value of 0.60 of shape index was also calculated which shows an asymmetric shape of the first-order decomposition kinetics of polyurethanes. The degree of conversion at the maximum reaction rate (α_m %) was calculated via simulation, and an average value of 60% was obtained (see Table II).¹² Figure 5 also shows the shape indices are 0.60, 1.15, and 1.57 for $n = 1, 2$ and 3, respectively.

Isothermal Condition

Decomposition Time

Integration of Eq. (2) gives the following expression if n is not equal to 1:

$$t = \frac{[(1 - \alpha)^{1-n} - 1]}{(n - 1)k} \quad (16)$$

Equation (2) can be rewritten after integration if n is equal to 1:

$$t = \frac{-\ln(1 - \alpha)}{k} \quad (17)$$

or

$$1 - \alpha = e^{-kt} \quad (18)$$

MDI Elastomer
Hard Segment 34 %
 5°C/minute under air

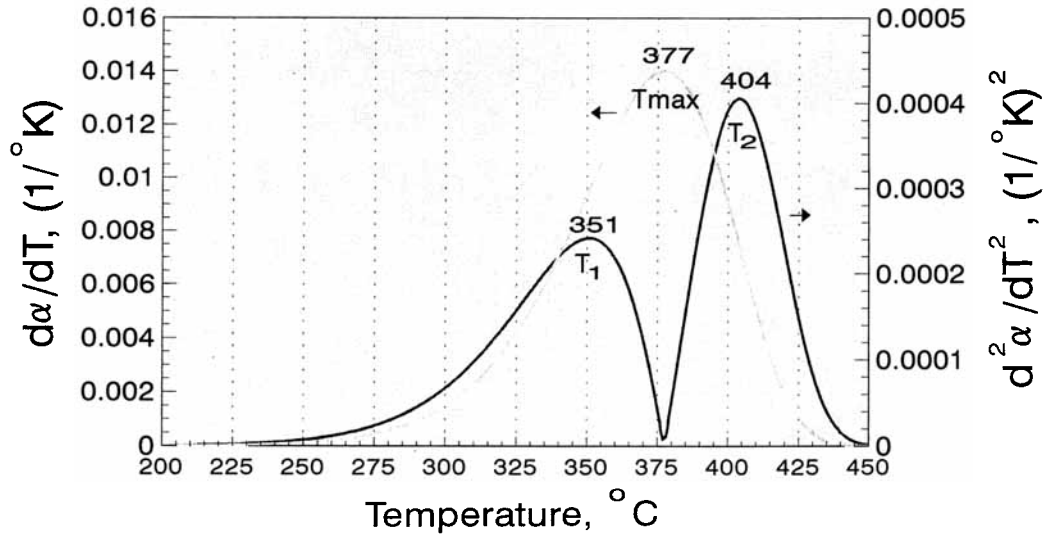


Figure 7 $d\alpha/dT$ and $d^2\alpha/dT^2$ vs. temperature.

Based on Eq. (18), $(1 - \alpha)$ % vs. time of the M34 elastomer is shown in Figure 8 via simulation. As can be seen, the decomposition at 300°C is much

faster than that at 240°C. We can also see that 60% of the M34 elastomer remained after 24 h at 240°C compared to 0% left at 280°C.

MDI Elastomer
Hard Segment 34 %
 Isothermal, under air

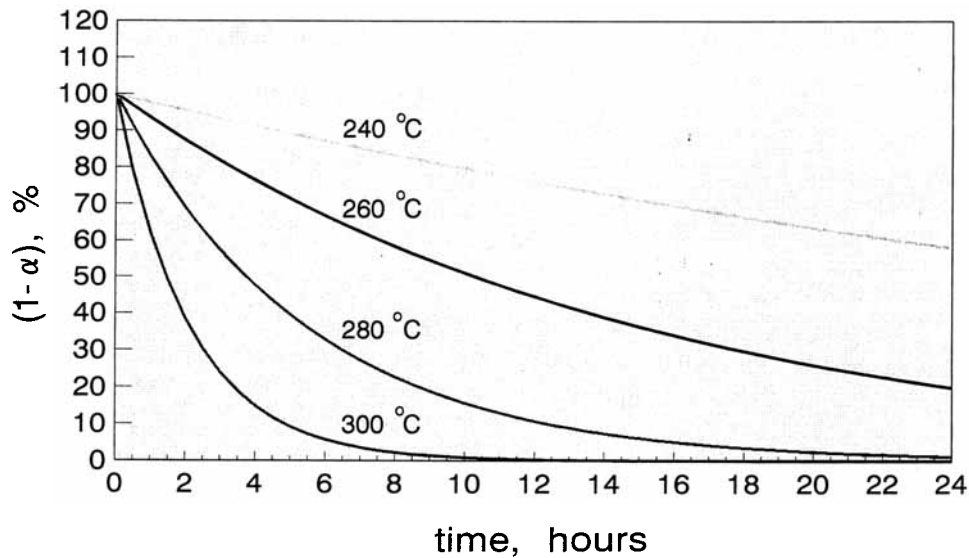


Figure 8 Isothermal curves at different temperatures.

Half-Life Time

After a specific period of time, $t_{1/2}$ = the half-life time, is defined as the value of α becomes 0.50. The half-life time can be expressed in the following equation if n is not equal to 1:

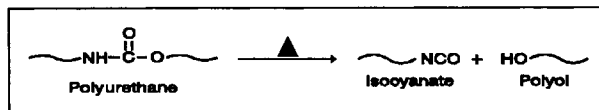
$$t_{1/2} = \frac{(0.5^{1-n} - 1)}{(n - 1)k} \quad (19)$$

The half-life time of $n = 1$ can be shown as follows:¹³

$$t_{1/2} = \frac{0.693}{k} \quad (20)$$

Because MDI-based elastomers exhibit the first-order kinetics of decomposition, the half-life time, $t_{1/2}$, and the decomposition rate constant, k , were calculated using the combination of Eqs. (3) and (20). The temperature functional curves are shown in Figure 9. When comparing the values of $t_{1/2}$ and k , the heat stability of MDI-based polyester elastomers with the different hard-segment contents decreases in the following order:

$$M24 > M34 > M50 > M100$$



This phenomenon can be explained as due to the heat instability of the urethane group in the structure that causes the dissociation at high temperature. M100 decomposed fastest due to the highest concentration of the urethane group.

Degree of Decomposition

Total time vs. temperature at different degrees of decomposition, using Eq. (17), can also be predicted and are shown in Figure 10. The relative time of different degrees of decomposition can be expressed in the following form after rearranging Eq. (17).

$$\frac{t_2}{t_1} = \frac{\ln(1 - \alpha_2)}{\ln(1 - \alpha_1)} \quad (21)$$

Lifetime

In order to calculate the estimated time of polyurethane elastomers to failure, a term called "lifetime," t_f , is defined when the degree of decomposition

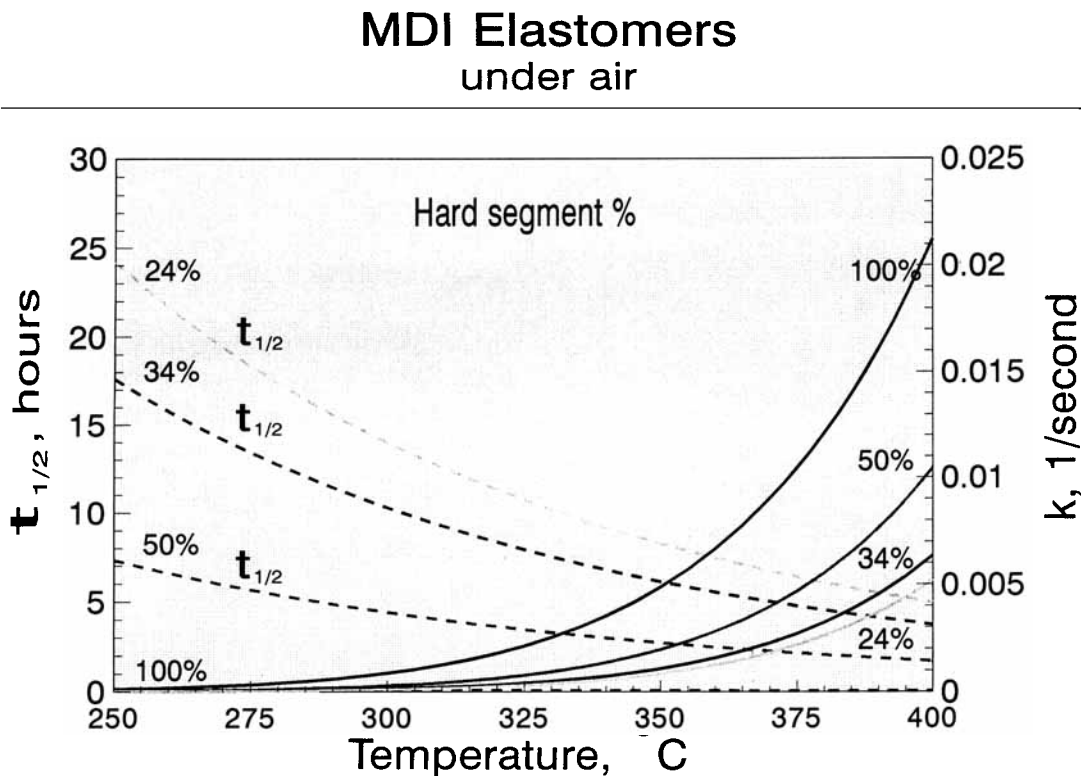


Figure 9 Decomposition rate constant and half-life time vs. temperature.

MDI Elastomer Hard Segment 34% under air

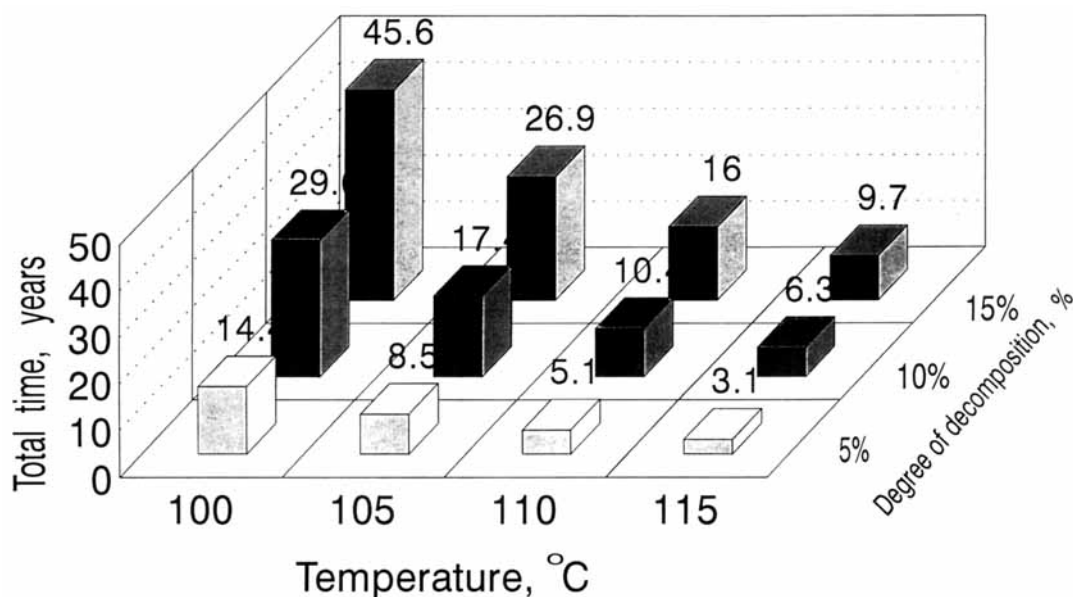


Figure 10 Total time vs. temperature at different degrees of decomposition.

reaches 5%, i.e., $1 - \alpha = 0.95$.¹⁴ Therefore, Eq. (16) can be rewritten if n is not equal to 1:

$$t_f = \frac{(0.95^{1-n} - 1)}{(n - 1)k} \quad (22)$$

Also, Eq. (17) can be rewritten if n is equal to 1:

$$t_f = \frac{0.0513}{k} \quad (23)$$

The predicted lifetime of polyurethane elastomers with different hard-segment contents can be cal-

culated using Eqs. (3) and (23) as well as the values of the activation energy and frequency factor listed in Table II. It can be seen very clearly from Table III that statically used polyurethane products at room temperature will last for several millennia without failure.

CONCLUSIONS

The activation energy and the frequency factor of polyurethane decomposition can be obtained by only one nonisothermal measurement of TGA. The same

Table III Predicted Lifetime of MDI-Based Elastomers Under Air

Temp., °C	Unit	M24	M34	M50	M100
25	millennium	704	342	40	1.7
80	century	2.5	1.4	0.3	0.02
100	decade	2.5	1.4	0.3	0.03
125	year	1.9	1.2	0.3	0.04
155	month	1.6	1.0	0.3	0.05
170	week	1.9	1.2	0.4	0.07
200	day	1.6	1.1	0.4	0.09
255	h	1.4	1.0	0.4	0.1

values of the activation energy and the frequency factor were obtained using the different constant heating rates under air for a 34% hard-segment elastomer (M34). The activation energy decreases as the hard-segment content of polyurethanes increases. The simulated curves can be drawn via mathematical treatment and a computer program. From the simulated method, T_m , T_1 , T_2 , T_2/T_1 , shape index, α_m %, $(1 - \alpha)_m$ %, and n can be calculated and compared. Also, the predicted lifetime, based upon thermal degradation, can be calculated at different temperatures. The calculations show that the polyurethane materials can be used at room temperature for several millennia without failure. It must be stressed that these calculations predict the expected lifetime of the polyurethane based upon thermal degradation only. Other factors such as hydrolysis, ultraviolet exposure, ozone concentration, and whether the elastomer is being used in a dynamic or static application will also affect the expected polyurethane lifetime. Comparison of the values of $t_{1/2}$, the heat stability of polyurethanes decreases in the following order:

$$M24 > M34 > M50 > M100$$

This phenomenon can be explained as due to the heat instability of the urethane group. The highest concentration of the urethane group in the M100 structure results in the worst heat stability.

The author wishes to express his indebtedness to T. Baranowski for his elastomer preparation as well as D. Anderson and J. Duffer for their TGA measurements.

REFERENCES

1. H. E. Kissinger, *Anal. Chem.*, **29**(11), 1702 (1957).
2. Z. S. Petrovic and Z. Z. Zavargo, *J. Appl. Polym. Sci.*, **32**, 4353 (1986).
3. J. Zsako, *J. Therm. Anal.*, **5**, 239 (1973).
4. J. V. Duffy, E. Hui, and B. Hartmann, *J. Appl. Polym. Sci.*, **33**, 2959 (1987).
5. P. S. Patel, P. P. Shah, and S. R. Patel, *Polym. Eng. Sci.*, **26**(17), 1186 (1986).
6. F. H. Sanchez and H. V. Torres, *J. Polym. Sci. Part A: Polym. Chem.*, **28**, 1579 (1990).
7. I. M. Salin and J. C. Seferis, *J. Appl. Polym. Sci.*, **47**, 847 (1993).
8. J. D. Nam and J. C. Seferis, *J. Polym. Sci. Part B: Polym. Phys.*, **29**, 601 (1991).
9. F. H. Sanchez and R. V. Graziano, *J. Appl. Polym. Sci.*, **46**, 571 (1992).
10. J. C. M. Torfs, L. Deij, A. J. Dorrepaal, and J. C. Heijens, *Anal. Chem.*, **56**(14), 2863 (1984).
11. C. F. Gerald, *Applied Numerical Analysis*, Addison-Wesley Publishing Company, Inc., Reading, MA, 1978.
12. H. H. Horowitz and G. Metzger, *Anal. Chem.*, **35**(10), 1464 (1963).
13. ASTM E 698-79.
14. C. D. Doyle, *J. Appl. Polym. Sci.*, **6**(24), 639 (1962).

Received February 14, 1994

Accepted March 31, 1994